Relativistic quasidegenerate perturbation theory with four-component general multiconfiguration reference functions

Makoto Miyajima, Yoshihiro Watanabe, and Haruyuki Nakano[a)]
Department of Chemistry, Graduate School of Sciences, Kyushu University, Fukuoka 812-8581, Japan

(Received 18 October 2005; accepted 23 November 2005; published online 23 January 2006)

Relativistic quasidegenerate perturbation theory (QDPT) using general multiconfiguration (GMC) reference functions is developed and implemented. It is the relativistic counterpart of the nonrelativistic QDPT with GMC reference and thus retains all the advantages of the nonrelativistic GMC reference QDPT, such as applicability to any configuration space and small computational cost compared to the complete configuration-space case. The method is applied to the potential-energy curves of the ground states of I_2 and Sb_2 molecules, the excitation energies of CH_3I, and the energies of the lowest terms of C, Si, and Ge atoms, and is shown to provide a balanced description of potential-energy curves and accurate transition energies for systems containing heavy elements and to provide much better results compared to the reference function (i.e., active space configuration interaction) level. © *2006 American Institute of Physics*.
[DOI: 10.1063/1.2161182]

I. INTRODUCTION

The importance of simultaneous consideration of relativistic and electron correlation effects for describing the electronic structures and chemical reactions of systems involving heavy atoms is now well recognized. Many methods for describing electronic structures, including the electron correlation effect, have been transferred to the four-component relativistic level: Møller-Plesset (MP) perturbation, configuration interaction (CI), coupled-cluster (CC) methods based on the Dirac-Hartree-Fock (DHF) wave function, and the Dirac-Kohn-Sham method. Multireference (MR) CI and CC methods are also available through relativistic program packages such as DIRAC (Ref. 1) and MOLFDIR.[2] However, as in the nonrelativistic case, the MRCI and MRCC methods require much computational cost. Lower cost multireference methods are needed.

In the nonrelativistic case, multireference perturbation theory (MRPT) based on multiconfiguration (MC) reference functions has become a basic and practical tool for studying the electronic structures of molecules and the potential-energy surfaces of chemical reactions. Several versions of MRPT are now included in various program packages such as GAMESS and MOLCAS. MRPT takes account of both static and dynamic electron correlations and thus can obtain accurate relative energies, including reaction, activation, and excitation energies, within a chemical accuracy (i.e., a few kcal/mol).

We have developed an MRPT using MC functions that we call "multiconfigurational quasidegenerate PT (MC-QDPT)."[3,4] It is a multiconfiguration basis *multi*-reference-state method based on van Vleck PT and includes multireference Møller-Plesset (MRMP) PT,[5–7] a *single*-reference-state method based on Rayleigh-Schrödinger PT, as a special case. In particular, a recently proposed version of MC-QDPT uses *general* multiconfiguration reference functions (GMC-QDPT or GMC-PT).[8,9] GMC-QDPT imposes no restriction on the reference space, so it is much more compact than complete-active-space-(CAS) based MRPT. In addition, since it can avoid unphysical multiple excitations, it is numerically stable. In this article, we describe the extension of GMC-QDPT to a relativistic version with four-component general MC reference functions.

Other versions of relativistic MRPTs have been already presented. Vilkas *et al.* proposed a relativistic MRMP method based on multiconfiguration Dirac-Fock reference functions.[10] Chaudhuri and Freed presented the relativistic effective valence shell (H^v) method.[11] These are relativistic generalizations of the nonrelativistic MRMP (Refs. 5–7) and H^v (Ref. 12) methods. Vilkas and Ishikawa further developed a generalized relativistic MRMP method based on MRCI reference functions.[13,14] However, their applications have been limited to atomic systems—no molecular applications have been reported so far to the best of our knowledge.

In Sec. II, we briefly review GMC-QDPT and describe the relativistic GMC-QDPT and its implementation. We describe the test applications of the scheme in Sec. III for the potential-energy curves of the ground states of I_2 and Sb_2 molecules, the excitation energies of methyl iodide CH_3I, and the energies of the lowest terms of C, Si, and Ge atoms. In Sec. IV, we summarize the main points and make some concluding remarks.

II. METHOD

A. QDPT with general multiconfiguration reference functions

We briefly review GMC-QDPT in this subsection. The effective Hamiltonian matrix to the second order $H_{\mathrm{eff}}^{(0-2)}$ of van Vleck perturbation theory with unitary normalization[15] is given by

[a)]Electronic mail: nakano@ccl.scc.kyushu-u.ac.jp

$$(H_{\mathrm{eff}}^{(0-2)})_{MN} = \langle \Phi_M^{(0)}|H|\Phi_N^{(0)}\rangle + \tfrac{1}{2}[\langle \Phi_M^{(0)}|HR_NH|\Phi_N^{(0)}\rangle + \langle \Phi_M^{(0)}|HR_MH|\Phi_N^{(0)}\rangle], \quad (1)$$

with

$$R_M = \sum_{I \notin \mathrm{Ref}} |\Phi_I^{(0)}\rangle (E_M^{(0)} - E_I^{(0)})^{-1} \langle \Phi_I^{(0)}|, \quad (2)$$

where $\Phi_M^{(0)}(\Phi_N^{(0)})$ and $\Phi_I^{(0)}$ are reference wave functions and a function in the complement space (Q) of the reference space (P), respectively, and $E_M^{(0)}$ and $E_I^{(0)}$ are zeroth-order energies of functions $\Phi_M^{(0)}$ and $\Phi_I^{(0)}$.

In GMC-QDPT, the reference wave functions $\mu(\nu)$ are determined by MC-self-consistent field (SCF) (or MC-CI) using general configuration space as an active (variational) space, where the *general configuration space* (GCS) is a space that is spanned by an arbitrary set of Slater determinants or configuration state functions (CSFs). Since the number of reference functions is usually equal to the number of target states, the dimension of reference (P) space is smaller (in many cases, much smaller) than that of GCS.

Taking the GCS-SCF or GCS-CI wave functions $\mu(\nu)$ as reference functions $\Phi_M^{(0)}(\Phi_N^{(0)})$, which define the P space, Eq. (1) becomes

$$(H_{\mathrm{eff}}^{(0-2)})_{\mu\nu} = E_\mu^{\mathrm{GCS\text{-}CI}} \delta_{\mu\nu} + \frac{1}{2}\left\{ \sum_{I \notin \mathrm{GCS}} \frac{\langle \mu|H|I\rangle\langle I|H|\nu\rangle}{E_\nu^{(0)} - E_I^{(0)}} + (\mu \leftrightarrow \nu)^* \right\}, \quad (3)$$

where I is now a determinant (or a CSF) outside the GCS (i.e., the active space). The notation $(\mu \leftrightarrow \nu)^*$ means interchange μ with ν and complex conjugation in the first term in the curly brackets. The complementary eigenfunctions of the GCS-CI Hamiltonian and the determinants (or CSFs) generated by exciting electrons out of the determinants (or CSFs) in GCS are orthogonal to the reference functions and define the Q space. The functions in the space complementary to the P space in GCS, however, do not appear in Eq. (3) since the interactions between the complementary functions and the reference functions are zero.

The third- and higher-order contributions are derived in the same manner,

$$(H_{\mathrm{eff}}^{(3)})_{\mu\nu} = \frac{1}{2}\left\{ \sum_{I,J \notin \mathrm{GCS}} \frac{\langle \mu|H|I\rangle\langle I|(V - E_\nu^{(1)})|J\rangle\langle J|H|\nu\rangle}{(E_\mu^{(0)} - E_I^{(0)})(E_\nu^{(0)} - E_J^{(0)})} + (\mu \leftrightarrow \nu)^* \right\}, \ldots, \quad (4)$$

though their computations are not very efficient compared to those for the second-order one, except for when the CI Hamiltonian matrix elements are readily available. The effective Hamiltonian to the second order is therefore mostly used for applications to molecular systems.

B. Relativistic GMC-QDPT and implementation

The relativistic molecular theory without spinor optimization can be derived along the same lines as in the nonrelativistic case if we begin with the no-virtual-pair Hamiltonian,

$$H_{\mathrm{DC}}^{+} = \Lambda^{+} H_{\mathrm{DC}} \Lambda^{+} (\Lambda^{+} = \mathcal{L}^{+}(1)\mathcal{L}^{+}(2)\cdots\mathcal{L}^{+}(N)), \quad (5)$$

for the Dirac-Coulomb Hamiltonian,

$$H_{\mathrm{DC}} = \sum_i h_{\mathrm{D}}(i) + \sum_{i>j} 1/r_{ij} \ (h_{\mathrm{D}}(i) = c\boldsymbol{\alpha}\cdot\mathbf{p} + \beta c^2 + V_{\mathrm{nuc}}), \quad (6)$$

where $\mathcal{L}^{+}(i)$ are the projection operators to electronic states i, $\boldsymbol{\alpha}$ and β are Pauli matrices in the usual relativistic theory, and $\mathbf{p}$ and V_{nuc} are momentum and nuclear attractive operators, respectively. We can also add the Breit Hamiltonian,

$$H_{\mathrm{B}} = -\sum_{i>j} \frac{1}{2r_{ij}} \left[\boldsymbol{\alpha}_i \cdot \boldsymbol{\alpha}_j + \frac{(\boldsymbol{\alpha}_i \cdot \mathbf{r}_{ij})(\boldsymbol{\alpha}_j \cdot \mathbf{r}_{ij})}{r_{ij}^2} \right], \quad (7)$$

to H_{DC} if necessary. Taking the second-quantized form of Eq. (5), we get

$$H_{\mathrm{DC}}^{+} = \sum_{pq} h_{pq} e_{pq} + \frac{1}{4}\sum_{pqrs} (pq \,\|\, rs) e_{pq,rs} = \sum_{pq} h_{pq} p^{+} q + \frac{1}{4}\sum_{pqrs} (pq \,\|\, rs) p^{+} r^{+} s q, \quad (8)$$

which is the starting point of the relativistic GMC-QDPT. The h_{pq} are one-electron integrals for operator $h_{\mathrm{D}}(i)$, and $(pq\|rs)$ are antisymmetrized two-electron integrals $[(pq\|rs) = (pq|rs) - (ps|rq)]$ for operator $1/r_{ij}$.

Applying the same treatment used for obtaining Eqs. (3) and (4) to the relativistic Hamiltonian, Eq. (8), we get a formal expression for the relativistic GMC-QDPT,

$$(H_{\mathrm{eff}})_{\mu\nu} = E_\mu^{\mathrm{GCS\text{-}CI}} \delta_{\mu\nu} + \frac{1}{2}\left\{ \sum_{I \notin \mathrm{GCS}} \frac{\langle \mu|H_{\mathrm{DC}}^{+}|I\rangle\langle I|H_{\mathrm{DC}}^{+}|\nu\rangle}{E_\nu^{(0)} - E_I^{(0)}} + \sum_{IJ \notin \mathrm{GCS}} \frac{\langle \mu|H_{\mathrm{DC}}^{+}|I\rangle\langle I|(V_{\mathrm{DC}}^{+} - E_\nu^{(1)})|J\rangle\langle J|H_{\mathrm{DC}}^{+}|\nu\rangle}{(E_\mu^{(0)} - E_I^{(0)})(E_\nu^{(0)} - E_J^{(0)})} + (\mu \leftrightarrow \nu)^* \right\} + \ldots. \quad (9)$$

Reference functions μ are expanded using single Slater determinants $|A\rangle$ as basis functions in our current implementation,

$$|\mu\rangle = \sum_{A \in \mathrm{GCS}} C_A^{\mu} |A\rangle. \quad (10)$$

Other basis sets using alpha and beta strings as used in the MRCI method by Fleig *et al.*[16] could also be used, but not implemented at present.

The second-order relativistic GMC-QDPT computation scheme is similar to that for nonrelativistic GMC-QDPT, which is described elsewhere.[8] We define the corresponding CAS (CCAS) as a CAS constructed from the same active electrons and spinors, that is, the minimal CAS that includes

the GCS, and divide the summation over I in Eq. (9) into summations over determinants outside CCAS and over the determinants outside the GCS but inside CCAS,

$$\sum_{I\notin \mathrm{GCS}} = \sum_{I\notin \mathrm{CCAS}} + \sum_{I\in \mathrm{CCAS}\wedge I\notin \mathrm{GCS}}. \tag{11}$$

Using this division, we can write the second-order term in the curly brackets in Eq. (9) as

$$(H^{(2)}_{\mathrm{eff}})_{\mu\nu} = \sum_{I\notin \mathrm{CCAS}} \frac{\langle \mu|H^{+}_{\mathrm{DC}}|I\rangle\langle I|H^{+}_{\mathrm{DC}}|\nu\rangle}{E^{(0)}_{\nu}-E^{(0)}_{I}} + \sum_{I\in \mathrm{CCAS}\wedge I\notin \mathrm{GCS}} \frac{\langle \mu|H^{+}_{\mathrm{DC}}|I\rangle\langle I|H^{+}_{\mathrm{DC}}|\nu\rangle}{E^{(0)}_{\nu}-E^{(0)}_{I}}. \tag{12}$$

The first term in Eq. (12) represents external excitations, while the second one represents internal excitations.

The external term can be expressed by

$$(H^{(2)}_{\mathrm{external}})_{\mu\nu} = \sum_{AB\in \mathrm{GCS}} C^{\mu^*}_{A} C^{\nu}_{B}\langle A|RH^{+}_{\mathrm{DC}}\frac{S}{E^{(0)}_{\nu}-H^{+(0)}_{\mathrm{DC}}}H^{+}_{\mathrm{DC}}R|B\rangle = \sum_{AB\in \mathrm{GCS}} C^{\mu^*}_{A} C^{\nu}_{B}\langle A|O^{(2)}|B\rangle, \tag{13}$$

where R and S are projectors onto the CCAS and its complementary space, respectively. Operator $O^{(2)}$ can be computed using the same diagrams used for the conventional QDPT with a CAS reference. Explicit formulas for this term are given in the Appendix. However, in GMC-QDPT [as well as in the original MC-QDPT (Ref. 3)] the rule for translating diagrams into mathematical expressions differs somewhat from that in conventional QDPT. The rule is described in detail elsewhere.[9]

In the diagrammatic computation of the effective Hamiltonian matrix, the key idea is the particle-hole formalism, as is well accepted.[17] In this formalism, particle-hole creation-annihilation operators b^+ and b are used instead of electron creation-annihilation operators a^+ and a,

$$\begin{aligned} &b^+ = a^+, \quad b = a \text{ for active and virtual spinors ("particles")},\\ &b^+ = a, \quad b = a^+ \text{ for core spinors ("hole")}, \end{aligned} \tag{14}$$

where the state with all the core spinors occupied by electrons is taken as the vacuum state. The Hamiltonian in normal form is expressed by

$$H^{+}_{\mathrm{DC}} = E_{\mathrm{core}} + \sum_{pq} f^{\mathrm{c}}_{pq}\{p^+q\} + \frac{1}{4}\sum_{pqrs}(pq\,\|\,rs)\{p^+r^+sq\}, \tag{15}$$

where E_{core} and f^{c}_{pq} are the core energy and core Fock matrix, respectively, and the curly brackets mean normal-ordered operators. This is the most commonly used expression.[17] However, we can use another definition of particle-hole operators,

$$\begin{aligned} &b^+ = a^+, \quad b = a \text{ for virtual spinors},\\ &b^+ = a, \quad b = a^+ \text{ for core and active spinors}, \end{aligned} \tag{16}$$

where the state with all the core and *active* spinors occupied by electrons is taken as the vacuum state. Holes in active spinors are treated as "quasiparticles," while, in the representation of Eq. (14), electrons in active spinors are treated as "quasiparticles." The Hamiltonian in normal form is given by

$$\begin{aligned} H^{+}_{\mathrm{DC}} &= E_{\mathrm{core+active}} + \sum_{pq} f^{\mathrm{ca}}_{pq}\{p^+q\} + \frac{1}{4}\sum_{pqrs}(pq\,\|\,rs)\{p^+r^+sq\}\\ &= E_{\mathrm{core+active}} + \sum_{pq}(-f^{\mathrm{ca}^*}_{pq})\{pq^+\}\\ &\quad + \frac{1}{4}\sum_{pqrs}(pq\,\|\,rs)^*\{prs^+q^+\}, \end{aligned} \tag{17}$$

where $E_{\mathrm{core+active}}$ and f^{ca}_{pq} are the energy and Fock matrix for the occupied core and active spinors, respectively, and the asterisks denote complex conjugation.

A diagrammatic expansion to obtain an explicit formula for the effective Hamiltonian can be done based on either Eq. (15) or (17). Since these equations are different expressions of the same Hamiltonian, they produced the same results. However, the computational cost is different in general. In the representation of Eq. (14), the computation is done with coupling coefficients $\langle I|p^+r^+\cdots sq|J\rangle$, where p, q, r, and s are labels of active spinors. In the representation of Eq. (16), coupling coefficients $\langle I|pr\cdots s^+q^+|J\rangle$ are used. Thus, if a coupling coefficient computation scheme such as the reduced intermediate space scheme of Zarrabian *et al.*[18] and Harrison and Zarrabian[19] is used, the formalism using Eqs. (14) and (15) is advantageous when the active spinors are filled with electrons less than the half number of active electrons, else the formalism using Eqs. (16) and (17) is advantageous. This is apparent from the fact that in these cases the reduced intermediate spaces are smaller than those in the opposite cases. While the scheme in our current code differs from Zarrabian *et al.* and Harrison and Zarrabian, there are some similarities. The explicit formulas used for practical computations are lengthy and therefore shown in the Appendix.

The internal term is computed with matrix operations for the Hamiltonian,

$$(H^{(2)}_{\mathrm{internal}})_{\mu\nu} = \sum_{I\in \mathrm{CCAS}\wedge I\notin \mathrm{GCS}} \times\left[\sum_{A\in \mathrm{GCS}} C^{\mu^*}_{A}(H^{+}_{\mathrm{DC}})_{AI}\bullet \sum_{B\in \mathrm{GCS}}\frac{(H^{+}_{\mathrm{DC}})_{IB}C^{\nu}_{B}}{E^{(0)}_{\nu}-E^{(0)}_{I}}\right]. \tag{18}$$

Matrix elements $(H^{+}_{\mathrm{DC}})_{AI}=\langle A|H^{+}_{\mathrm{DC}}|I\rangle$ $((H^{+}_{\mathrm{DC}})_{IB}=\langle I|H^{+}_{\mathrm{DC}}|B\rangle)$ may be readily available for the determinants in CCAS. The computational cost compared to the external term is negligible in most cases.

III. APPLICATIONS

We applied the present method to some molecular systems to illustrate its performance. We calculated the potential-energy curves (PECs) of the ground state of the I_2 and Sb_2 molecules, the excitation energies of CH_3I, and the energies of the lowest terms of the C, Si, and Ge atoms. Dirac-Coulomb and Dirac-Coulomb-Breit Hamiltonians

TABLE I. Bond length, vibrational frequency, and dissociation energy for I_2 molecule.

Method	r_e/Å	ω_e/cm^{-1}	D_e/eV
DHF	2.69	221	···
MP2	2.67	211	···
GCS-CI(10,12)	2.75	168	0.83
GMC-PT(10,12)	2.70	205	1.39
GCS-CI(10,24)	2.78	163	1.01
GMC-PT(10,24)	2.70	205	1.38
FSCCSD[a]	2.69	214	1.47
Expt.[b]	2.67	214.5	1.56

[a]Reference 24.
[b]Reference 23.

were used for the molecules and for the atoms, respectively, and the spinors were determined with the Dirac-Hartree-Fock method using DIRAC (Ref. 1) (for CH_3I), MOLFDIR (Ref. 2) (for C, Si, and Ge), and the REL4D program[20] of UTCHEM (Ref. 21) (for I_2 and Sb_2).

A. Potential-energy curves of I_2 and Sb_2 molecules

We calculated the potential-energy curves of the ground states ($X0_g^+$) of I_2 and Sb_2 molecules, which are examples of single- and triple-bond dissociations, respectively. Two active spaces were taken for each molecule. The one for I_2 was spanned by the determinants of which weights in the CAS(10,12) CI wave function were greater than 10^{-8} (i.e., $|C_I| > 10^{-4}$) and the other for I_2 was obtained using CAS(10,24) instead of CAS(10,12), where CAS(n,m) means the complete active space constructed from n electrons and m spinors. These GCSs are referred to as GCS(10,12) and GCS(10,24). The active spaces for Sb_2 were similar to those for I_2, that is, the spaces spanned by the determinants selected from the CAS(6,12) and CAS(6,24) CI wave functions [GCS(6,12) and GCS(6,24)]. The 12 spinors in CAS(n,12) roughly correspond to 5p orbitals, and the additional 12 spinors in CAS(n,24) roughly correspond to diffuse p orbitals for flexibility of active spaces. The electrons in the lowest 56 spinors were not correlated (56 frozen-core spinors) in the perturbation calculations for both molecules. We used Dyall's VTZ basis set.[22]

Table I summarizes the calculated spectroscopic constants for I_2. All the constants, r_e, ω_e, and D_e, of GMC-PT were in good agreement with the experimental values.[23] (In this subsection, GMC-PT is used because the reference states are single.) At the GCS-CI (i.e., reference function) level, the differences from the experimental values for r_e, ω_e, and D_e were 0.11 (0.08) Å, 51.5(46.5) cm^{-1}, and 0.55 (0.73) eV, respectively, for GCS(10,24) [GCS(10,12)]. At the GMC-PT level, the differences were reduced to 0.03 (0.03) Å, 9.5(9.5) cm^{-1}, and 0.17 (0.18) eV, respectively. The results of the Fock-space coupled-cluster method singles and doubles (FSCCSD) method are also listed in Table I. FSCCSD yielded very accurate values.[24] The error trends of GMC-PT and FSCCSD (overestimation for r_e and underestimation for ω_e and D_e) were similar, and thus the values produced by these methods were rather close.

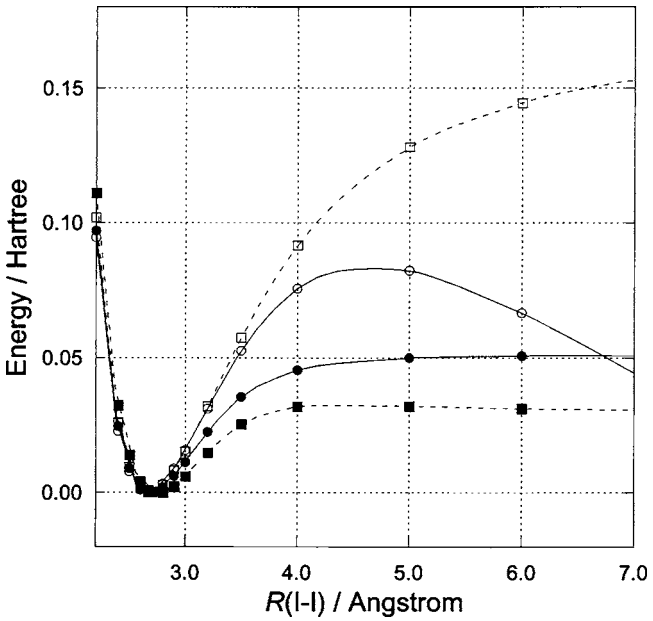

FIG. 1. DHF(□), MP2(◯), GCS-CI(■), and GMC-PT(●) potential-energy curves of the ground ($X0_g^+$) states of I_2. Active space GCS(10,12) was used for GCS-CI and GMC-PT.

Figures 1 and 2 show the ground-state PECs for the I_2 molecule obtained with second-order relativistic GMC-PT using GCS(10,12) and GCS(10,24), respectively. The curves for DHF, second-order Møller-Plesset (MP2) PT, and GCS-CI are also shown for comparison. The performance of the DHF and MP2 methods for radical breaking was similar to that of the corresponding nonrelativistic methods, that is, a good description in the equilibrium distance region and a poor one in the large bond distance region. In contrast, GCS-CI gave a qualitatively correct dissociation limit, and GMC-PT gave a quantitatively good description for the

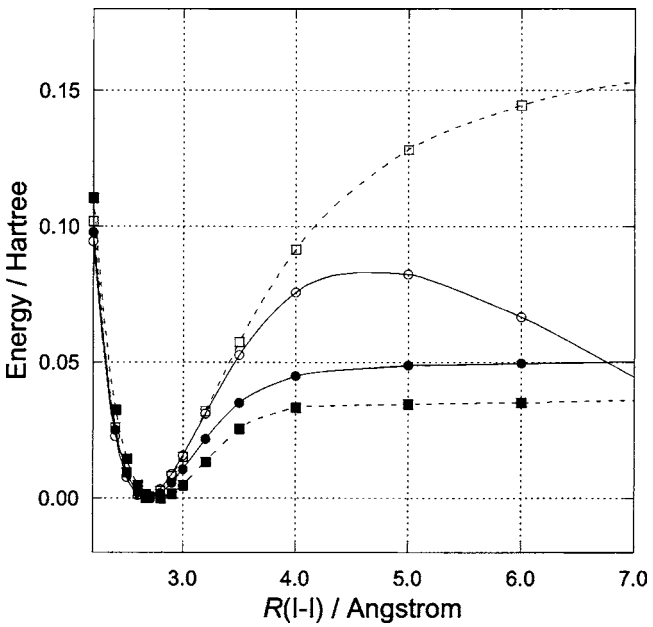

FIG. 2. DHF(□), MP2(◯), GCS-CI(■), and GMC-PT(●) potential-energy curves of the ground ($X0_g^+$) states of I_2. Active space GCS(10,24) was used for GCS-CI and GMC-PT.

TABLE II. Bond length, vibrational frequency, and dissociation energy for Sb_2 molecule.

Method	r_e/Å	ω_e/cm^{-1}	D_e/eV
DHF	2.45	340	···
MP2	2.52	283	···
GCS-CI(6,12)	2.56	219	2.09
GMC-PT(6,12)	2.53	273	2.64
GCS-CI(6,24)	2.56	225	2.31
GMC-PT(6,24)	2.54	279	2.63
MRSDCI/RCI[a]	2.59	246	1.86
Expt.[b]	2.34	270	3.09

[a]Reference 25.
[b]Reference 23.

whole region, as the spectroscopic constants indicate. The effect of the active space was very small at the GMC-PT level.

Table II shows the spectroscopic constants of Sb_2, and Figs. 3 and 4 show the ground-state PECs. The behaviors of the methods were similar to those for the I_2 molecule. However, the differences for the spectroscopic constants were larger. The equilibrium nuclear distance at the GCS-CI level was 2.56 Å for both GCS(6,12) and GCS(6,24), 0.22 Å larger than the experimental value, 2.34 Å. This distance was not fully recovered at the GMC-PT level; it was still 0.18 (0.19) Å larger for GCS(6,24) [GCS(6,12)]. This was also the case at the MP2 level, which gave a similar r_e of 2.52 Å. The difference between GMC-PT and the experimental values in dissociation energy was also not small: 0.46 (0.45) eV larger than the experimental value, 3.09 eV, for GCS(6,24) [GCS(6,12)]. However, these features were not the only ones of the relativistic GMC-PT. A two-component method MRSDCI/RCI gave a 0.25 Å longer distance and a 1.23 eV larger dissociation energy.[25] Furthermore, scalar (one-component) GMC-PT with GCS(6,24) using the Martin/Sundermann Stuttgart relativistic, large core valence triple-zeta effective core potential basis set[26,27] gave 2.56 Å, 221 cm^{-1}, and 2.08 eV. We do not pursue this issue further since the Sb_2 calculations were a part of the test applications.

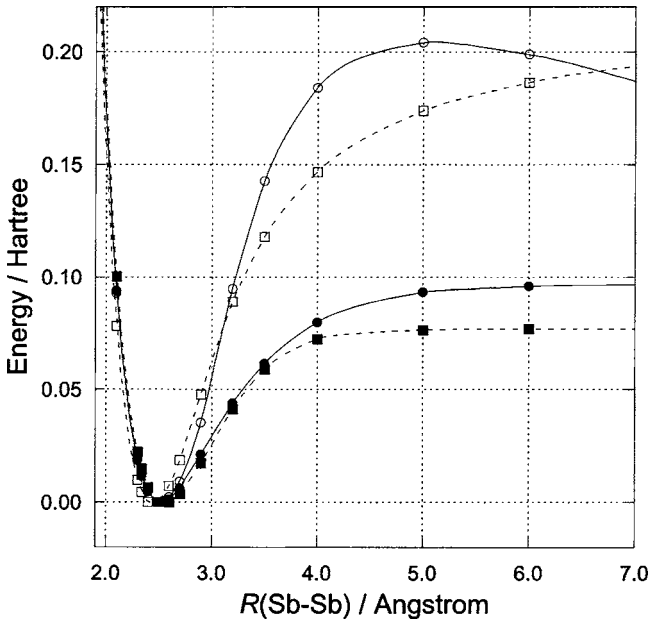

FIG. 3. DHF(□), MP2(◯), GCS-CI(■), and GMC-PT(●) potential-energy curves of the ground ($X0_g^+$) states of Sb_2. Active space GCS(6,12) was used for GCS-CI and GMC-PT.

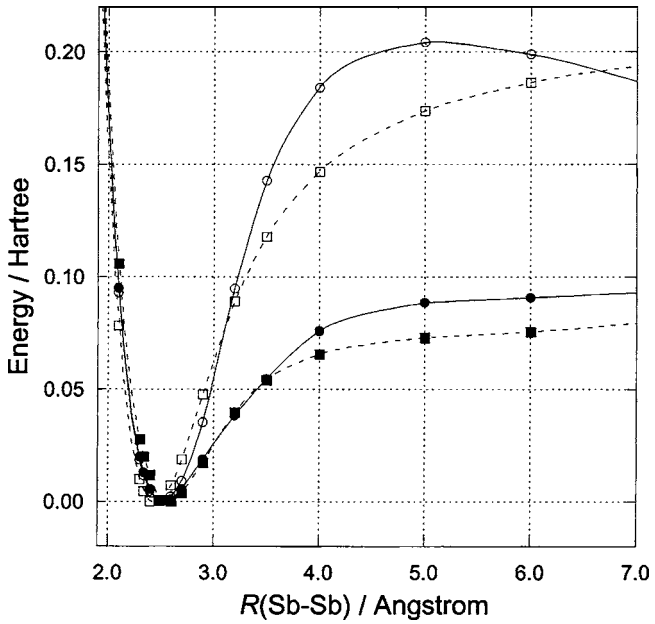

FIG. 4. DHF(□), MP2(◯), GCS-CI(■), and GMC-PT(●) potential-energy curves of the ground ($X0_g^+$) states of Sb_2. Active space GCS(6,24) was used for GCS-CI and GMC-PT.

The selection of Slater determinants based on the CAS-CI coefficients means that different active spaces are taken depending on the molecular geometry, and this may cause PEC discontinuity. However, if a suitably small threshold is chosen, the PECs are mostly smooth, and the advantage of reducing the computational cost is much larger than the disadvantage. Based on our experience, a threshold between 10^{-4} and 10^{-3} is appropriate for $|C_I|$. In the present calculations, we used 10^{-4} to be on the safe side.

B. Excitation energies of methyl iodide CH_3I

In our calculations of the excitation energies of methyl iodide CH_3I, we used target states of $1E$, $2E$, $3E$, $1A_2$, and $2A_1$ states, which come mainly from n to σ^* single excitations. The basis set used was a valence triple-zeta plus double polarization basis set. The valence functions were contracted from the uncontracted relativistic Gaussian-type functions basis set by Koga *et al.*,[28] and the polarization functions were taken from Dunning's correlation consistent polarized valence triple-zeta (cc-pVTZ) basis set.[29] Three active spaces (GCS I-III) were tested: MRSD- (GCS I) and MRS-type (GCS II and III), that is, spaces spanned by parent configurations plus singles and doubles (GCS I) and parent configurations plus singles (GCS II and III), where singles and doubles were made within the active-spinor space. One DHF configuration, four HOMO-LUMO configurations, and four second-HOMO-LUMO configurations were used as the parent configurations. The singles and doubles in space I were constructed from 12 electrons and 20 spinors, corre-

TABLE III. Vertical excitation energies of methyl iodide CH_3I in eV.

	GCS I[a]		GCS II[b]		GCS III[c]			
State	GCS-CI	GMC-QDPT	GCS-CI	GMC-QDPT	GCS-CI	GMC-QDPT	SO-MCQDPT[d]	Expt.[e]
$1E$	4.87	4.09	4.73	4.06	4.45	4.07	4.16	4.13
$2E$	5.06	4.26	4.92	4.23	4.63	4.23	4.30	···
$1A_2$	5.47	4.65	5.33	4.62	5.02	4.63	4.65	···
$2A_1$	5.56	4.71	5.44	4.67	5.13	4.68	4.69	4.75
$3E$	5.93	5.06	5.80	5.03	5.50	5.05	5.03	5.17

[a]MRSD active space constructed from 12 electrons and 20 spinors.
[b]MRS active space constructed from 12 electrons and 24 spinors.
[c]MRS active space constructed from 12 electrons and 36 spinors.
[d]Reference 30.
[e]Reference 32.

sponding to carbon $2s$ and $2p$, hydrogen $1s$, and iodine $5p$ orbitals. The singles in GCS II (III) were constructed from 12 electrons and 24 (36) spinors, where more spinors had been included to take the spinor optimization effect into account instead of the electron correlation effect by doubles. The lowest 30 spinors were frozen in the perturbation calculations.

The computed excitation energies are summarized in Table III. The spin-orbit (SO) MCQDPT results[30] are also listed for comparison. SO-MCQDPT (Ref. 31) is a two-component multireference multistate perturbation method proposed by Fedorov and Finley. At the GCS-CI (i.e., reference function) level, the deviations in excitation energies among the three active spaces were somewhat large. In contrast, at the GMC-QDPT level, they were very close to each other, regardless of the active spaces. The largest deviation was only 0.04 eV, indicating that, at the GCS-CI level, the description level differed depending on the active spaces, while, at the GMC-QDPT level, the balance of the description was well recovered.

The experimental results of magnetic circular dichroism are available for $1E$, $2A_1$, and $3E$ states,[32] and they are also listed in Table III. We can see that GMC-QDPT reproduced the experimental values well. Taking the results for space I as an example, we can see that the deviations from the experimental values were 0.04, 0.04, and 0.11 eV for the $1E$, $2A_1$, and $3E$ states, respectively.

Table IV shows the approximate weight of the reference function occupied in the first-order perturbed wave function,

$$W_{\mathrm{ref}} = \left[1 + \sum_{\mu} |D_{\mu}|^2 \langle \Psi_{\mu}^{(1)} | \Psi_{\mu}^{(1)} \rangle \right]^{-1} \simeq \langle \Psi_{\mathrm{ref}} | \Psi_{\mathrm{ref}} \rangle / \langle \Psi_{\mathrm{ref}} + \Psi^{(1)} | \Psi_{\mathrm{ref}} + \Psi^{(1)} \rangle, \tag{19}$$

with

$$\Psi_{\mathrm{ref}} = \sum_{\mu} D_{\mu} \Psi_{\mu}^{\mathrm{ref}}, \quad \Psi^{(1)} = \sum_{\mu} D_{\mu} \Psi_{\mu}^{(1)}, \tag{20}$$

where $\Psi_{\mu}^{\mathrm{ref}} (= |\mu\rangle)$ and $\Psi_{\mu}^{(1)}$ are the reference and first-order wave functions for state μ, respectively, and $\{D_{\mu}\}$ is the eigenvector of the effective Hamiltonian matrix $(H_{\mathrm{eff}}^{(0-2)})_{\mu\nu}$ for state μ. The weight, W_{ref}, is a measure of the quality of the reference wave functions, and the relative weight calculated for different states gives a measure of the balance of the calculation.

The nonreference weight, $(1 - W_{\mathrm{ref}})$, can be further decomposed into pure internal, internal, and external weights, where the pure internal weight means the contribution from the active- to active-spinor excitations not included in the

TABLE IV. Reference and SD configurations weights in the first-order GMC-QDPT wave function in percent.

	GCS I		GCS II		GCS III	
State	Ref.	SD[a]	Ref.	SD[a]	Ref.	SD[a]
$1A_1$	89.3	10.7 (0.0+0.1+10.6)	88.8	11.2 (0.8+0.1+10.3)	88.9	11.1 (2.2+0.3+8.6)
$1E$	85.5	14.5 (0.0+0.1+14.4)	85.4	14.6 (0.6+0.1+13.9)	87.7	12.3 (2.1+0.3+9.9)
$2E$	85.5	14.5 (0.0+0.1+14.4)	85.3	14.7 (0.6+0.1+14.0)	87.6	12.4 (2.2+0.4+9.8)
$1A_2$	85.1	14.9 (0.0+0.1+14.8)	84.9	15.1 (0.6+0.1+14.4)	87.6	12.4 (2.1+0.4+9.9)
$2A_1$	85.2	14.8 (0.0+0.1+14.7)	84.9	15.1 (0.7+0.1+14.3)	87.4	12.6 (2.3+0.3+10.0)
$3E$	85.4	14.6 (0.0+0.2+14.4)	85.2	14.8 (0.6+0.2+14.0)	87.3	12.7 (2.2+0.5+10.0)

[a]The three numbers in parentheses in the SD configurations weight indicate pure internal, internal, and external excitation weights (see the text for more details).

TABLE V. Energies of the lowest terms of C, Si, and Ge atoms in cm^{-1}. The values in the parentheses are the errors in percent from experimental values.

Term	GCS-CI	GMC-QDPT	SO-MCQDPT[a]	Expt.[b]
		C		
$^3P_0$	0	0	0	0
$^3P_1$	15.48(−5.6)	15.69(−4.3)	13.27(−19.1)	16.40
$^3P_2$	40.49(−6.7)	41.56(−4.2)	39.57(−8.8)	43.40
$^1D_2$	12 798.92(25.6)	10 323.98(1.3)	10250.81(0.6)	10 192.63
$^1S_0$	20 952.87(−3.2)	21 041.33(−2.8)	21106.28(−2.5)	21 648.01
		Si		
$^3P_0$	0	0	0	0
$^3P_1$	71.78(−6.9)	74.55(−3.3)	62.33(−19.2)	77.11
$^3P_2$	208.06(−6.8)	215.63(−3.4)	181.26(−18.8)	223.16
$^1D_2$	8 586.97(36.3)	6 378.96(1.3)	6 284.01(−0.2)	6 298.85
$^1S_0$	14 882.64(−3.3)	14 904.32(−3.2)	14 752.15(−4.2)	15 394.36
		Ge		
$^3P_0$	0	0	0	0
$^3P_1$	455.95(−19.2)	532.61(−4.4)	443.92(−20.3)	557.13
$^3P_2$	1 170.59(−17.0)	1343.99(−4.7)	1 152.07(−18.3)	1 409.96
$^1D_2$	9 172.17(28.7)	7197.43(1.0)	7 118.54(−0.1)	7 125.30
$^1S_0$	16 528.28(1.0)	16001.39(−2.2)	16 286.67(−0.5)	16 367.33

[a]Reference 31.
[b]Reference 36.

GCS, the internal weight means the core- to active-spinor excitations, and the external weight means the contribution from the excitations involving virtual spinors. These numbers are also listed (in parentheses) in Table IV.

From Table IV we can see that the reference weights were fairly large, about 85% (84.9%-89.3%), and the differences between the ground and excited states in the same active space were small ($\Delta W_{\mathrm{ref}}^{\max}=4.2\%$, 3.9%, and 1.6% for GCS I, II, and III, respectively). This means that the qualities of the wave functions were similar, i.e., well balanced, between the ground state and excited states, which supports our excitation energy results. The slightly larger weights of the ground state were due to the use of spinors optimized for the ground state. One more feature we can see from the table is that the pure internal contribution was very small (less than 1%) except for GCS III, which includes relatively many active spinors. This validates our choice of active spaces.

C. Energy of the lowest terms of carbon, silicon, and germanium atoms

As a final example, we calculated the lowest terms of group IV atoms, C, Si, and Ge. We included the Breit interaction in the Hamiltonian since the magnetic terms are important for obtaining accurate spin-orbit splitting. The basis sets used were the uncontracted relativistic Gaussian-type function basis sets by Koga *et al.*,[28] augmented by *d* and *f* polarization functions taken from Dunning *et al.* augmented cc-pVTZ basis set.[33–35] The spinors were optimized using the open-shell DHF method with two electrons in six spinors. The active spaces were constructed from four electrons and 16 spinors (double valence spinor space) in all atoms, and, as in the calculations of I_2 and Sb_2, only determinants satisfying $|C_I|>10^{-4}$ for at least one of the $^3P_0$, $^3P_1$, $^3P_2$, $^1D_2$, and $^1S_0$ states were included in the active space [GCS(4,16)]. The *K*-shell spinors of C, the *K*- and *L*-shell spinors of Si, and the *K*-, *L*-, and *M*-shell spinors of Ge were frozen in the perturbation calculation.

The results are listed in Table V. The GMC-QDPT results were in very good agreement with the experimental values.[36] The average and maximum errors were only 3.0% and 4.7%, respectively. The GCS-CI results were also close to the experimental values, except for the $^1D_2$ state, for which the error was 25.6%-36.3%. GMC-QDPT provided better results than the GCS-CI in almost all the cases. SO-MCQDPT also gave very good results, especially for the $^1D_2$ and $^1S_0$ states.[31] However, for the spin-orbit splitting for the ^3P states, GMC-QDPT yielded better results. The maximum error of SO-MCQDPT for these states was 20.3% whereas that of GMC-QDPT was 4.7%.

We also performed wave-function analysis using the reference weights for these atoms. In all the atoms, the approximate reference weights exceeded 90% (96.2%-96.8% for C, 93.3%-94.3% for Si, and 91.3%-92.3% for Ge), and the differences between the states were very small, which supports the accuracy of our results.

IV. CONCLUSION

We have described relativistic GMC-QDPT, i.e., an extension of nonrelativistic GMC-QDPT to a relativistic version with four-component general MC reference functions. It retains the advantages of the nonrelativistic GMC-QDPT: flexible selection of configuration spaces, avoidance of unphysical multiple excitations, efficient computation using both diagrammatic and CI-matrix based methods, etc.

We applied our scheme to the calculations of the potential-energy curves of I_2 and Sb_2 molecules, the excitation energies of CH_3I, and the energies of the lowest terms of

C, Si, and Ge atoms. Except for the Sb_2 case, the present method gave results close to the experimental values and comparable to the results of other highly correlated relativistic methods such as the Fock-space coupled-cluster method and the spin-orbit MC-QDPT. Wave-function analysis supported our calculations. The reference weights were all large, and their deviations were small, which indicates the high quality and good balance of the calculations.

The multipartitioning Hamiltonian approach,[37,38] which allows different partitioning for different states and thus is more flexible than the present method, and the intruder state avoidance approach[39] have also been implemented and are now available. Although these approaches, using a different Hamiltonian partitioning, are not in the framework of GMC-QDPT, they can be easily included with small changes as options at the program level.

ACKNOWLEDGMENTS

The present research was supported in part by a Grant-in-Aid for Scientific Research (Division B) from the Japan Society for the Promotion of Science and in part by CREST from Japan Science and Technology Agency.

APPENDIX: EXPLICIT FORMULAS FOR EXTERNAL TERM OF SECOND-ORDER RELATIVISTIC GMC-QDPT

In the text, explicit formulas are not given for the external term, Eq. (13), of the effective Hamiltonian matrix. Here we present formulas that can be used for practical computation of second-order relativistic GMC-QDPT for the reader's convenience. The formulas are similar to those for nonrelativistic MC-QDPT,[3] but somewhat different, particularly if we use the representation given by Eq. (16).

We have two formulas. One is for the common representation, Eq. (14), and the other is for the less common representation, Eq. (16). We present the one for Eq. (16) first.

The external term is expressed by zero- to three-body terms,

$$(H^{(2)}_{\text{external}})_{\mu\nu} = K^{0\text{-body}}_{\mu\nu} + K^{1\text{-body}}_{\mu\nu} + K^{2\text{-body}}_{\mu\nu} + K^{3\text{-body}}_{\mu\nu},$$

with

$$K^{0\text{-body}}_{\mu\nu} = \sum_{B\in\text{GCS}} C_B^{\mu *} C_B^{\nu} \sum_{m=1}^{2} O_m,$$

$$K^{1\text{-body}}_{\mu\nu} = -\sum_{Be\text{GCS}} \sum_{pq\in\text{act}} \langle\mu|qp^+|B\rangle C_B^{\nu} \sum_{m=1}^{6} S_m,$$

$$K^{2\text{-body}}_{\mu\nu} = \sum_{B\in\text{GCS}} \sum_{pqrs\in\text{act}} \langle\mu|qsr^+p^+|B\rangle C_B^{\nu} \sum_{m=1}^{7} D_m,$$

and

$$K^{3\text{-body}}_{\mu\nu} = -\sum_{B\in\text{GCS}} \sum_{pqrstu\in\text{act}} \langle\mu|qsut^+r^+p^+|B\rangle C_B^{\nu} \sum_{m=1}^{2} T_m.$$

The zero- to three-body terms are composed of the following terms

(a) Zero-body terms

$$O_1 = -\sum_{i\in\text{core,act}} \sum_{e\in\text{vir}} \frac{(ie)(ei)}{\varepsilon_e - \varepsilon_i + \Delta E_{B\nu}},$$

$$O_2 = -\frac{1}{4} \sum_{ij\in\text{core,act}} \sum_{ef\in\text{vir}} \frac{(ie\,\|\,jf)(ei\,\|\,fj)}{\varepsilon_e - \varepsilon_i + \varepsilon_f - \varepsilon_j + \Delta E_{B\nu}}.$$

(b) One-body terms

$$S_1 = -\sum_{e\in\text{vir}} \frac{(pe)(eq)}{\varepsilon_e - \varepsilon_q + \Delta E_{B\nu}},$$

$$S_2 = \sum_{i\in\text{core}} \frac{(iq)(pi)}{\varepsilon_p - \varepsilon_i + \Delta E_{B\nu}},$$

$$S_3 = -\sum_{i\in\text{core,act}} \sum_{e\in\text{vir}} \frac{(ie)(ei\,\|\,pq)}{\varepsilon_e - \varepsilon_i + \varepsilon_p - \varepsilon_q + \Delta E_{B\nu}},$$

$$S_4 = -\sum_{i\in\text{core,act}} \sum_{e\in\text{vir}} \frac{(pq\,\|\,ie)(ei)}{\varepsilon_e - \varepsilon_i + \Delta E_{B\nu}},$$

$$S_5 = \frac{1}{2} \sum_{i\in\text{core,act}} \sum_{ef\in\text{vir}} \frac{(pe\,\|\,if)(ei\,\|\,fq)}{\varepsilon_e - \varepsilon_i + \varepsilon_f - \varepsilon_q + \Delta E_{B\nu}},$$

$$S_6 = -\frac{1}{2} \sum_{ij\in\text{core,act}} \sum_{e\in\text{vir}} \frac{(iq\,\|\,je)(ei\,\|\,pj)}{\varepsilon_e - \varepsilon_i + \varepsilon_p - \varepsilon_j + \Delta E_{B\nu}}.$$

(c) Two-body terms

$$D_1 = -\frac{1}{2} \sum_{e\in\text{vir}} \frac{(pe)(eq\,\|\,rs)}{\varepsilon_e - \varepsilon_q + \varepsilon_r - \varepsilon_s + \Delta E_{B\nu}},$$

$$D_2 = \frac{1}{2} \sum_{i\in\text{core}} \frac{(iq)(pi\,\|\,rs)}{\varepsilon_p - \varepsilon_i + \varepsilon_r - \varepsilon_s + \Delta E_{B\nu}},$$

$$D_3 = -\frac{1}{2} \sum_{e\in\text{vir}} \frac{(pq\,\|\,re)(es)}{\varepsilon_e - \varepsilon_s + \Delta E_{B\nu}},$$

$$D_4 = \frac{1}{2} \sum_{i\in\text{core}} \frac{(pq\,\|\,is)(ri)}{\varepsilon_r - \varepsilon_i + \Delta E_{B\nu}},$$

$$D_5 = -\frac{1}{8} \sum_{ef\in\text{vir}} \frac{(pe\,\|\,rf)(eq\,\|\,fs)}{\varepsilon_e - \varepsilon_q + \varepsilon_f - \varepsilon_s + \Delta E_{B\nu}},$$

$$D_6 = -\sum_{i\in\text{core,act}} \sum_{e\in\text{vir}} \frac{(pq\,\|\,ie)(ei\,\|\,rs)}{\varepsilon_e - \varepsilon_i + \varepsilon_r - \varepsilon_s + \Delta E_{B\nu}},$$

$$D_7 = -\frac{1}{8} \sum_{ij\in\text{core,act}}{}^{*} \frac{(iq\,\|\,js)(pi\,\|\,rj)}{\varepsilon_p - \varepsilon_i + \varepsilon_r - \varepsilon_j + \Delta E_{B\nu}}.$$

(d) Three-body terms

$$T_1 = -\frac{1}{4} \sum_{e\in\text{vir}} \frac{(pq\,\|\,re)(es\,\|\,tu)}{\varepsilon_e - \varepsilon_s + \varepsilon_t - \varepsilon_u + \Delta E_{B\nu}},$$

$$T_2 = \frac{1}{4} \sum_{i \in \text{core}} \frac{(pq \| is)(ri \| tu)}{\varepsilon_r - \varepsilon_i + \varepsilon_t - \varepsilon_u + \Delta E_{B\nu}}.$$

Summation symbol Σ^* in D_7 means that the summation for the ij pair is taken so that at least one of i or j is a core-spinor label. The symbol (pq) denotes the Fock matrix,

$$(pq) = f_{pq}^{\text{ca}} = h_{pq} + \sum_{i \in \text{core,act}} (pq \| ii).$$

The $\Delta E_{B\nu}$ represents the energy differences of zeroth-order configuration B and reference state μ,

$$\Delta E_{B\nu} = E_B^{(0)} - E_\nu^{(0)} = \sum_{p \in \text{act}} [\langle B|p^+p|B\rangle - \langle \nu|p^+p|\nu\rangle].$$

The computation is done using the coupling coefficient driven method. These coupling coefficients are sparse and can be prescreened based on the condition $\langle \mu|qs\cdots r^+p^+|B\rangle C_B^\nu > \delta$, where $\delta = 10^{-9}$ is usually sufficient to keep the energy accuracy better than 10^{-5} hartree.

The formula for Eq. (14) can be obtained with the following changes.

(1) Fock matrix

$$(pq) = f_{pq}^{c} = h_{pq} + \sum_{i \in \text{core}} (pq \| ii).$$

(2) Coupling coefficients

$$\langle \mu|qp^+|B\rangle \rightarrow -\langle \mu|p^+q|B\rangle,$$

$$\langle \mu|qsr^+p^+|B\rangle \rightarrow \langle \mu|p^+r^+sq|B\rangle,$$

$$\langle \mu|qsut^+r^+p^+|B\rangle \rightarrow -\langle \mu|p^+r^+t^+usq|B\rangle.$$

(3) Spinor summation. In the summations in O_m, S_m, D_m, and T_m above, labels i and j run over core and active spinors, and labels e and f run over virtual spinors. This should be changed so that summation i and j run over only core spinors and summation e and f run over both active and virtual spinors. However, as in O_m, S_m, D_m, and T_m above, the summations are so restricted that at least one label must include a core or virtual label to avoid internal (active to active) excitations.

Finally the multipartitioning Hamiltonian approach[37,38] described in Sec. IV can be implemented simply by changing the spinor energies in O_m, S_m, D_m, and T_m, as well as $\Delta E_{B\nu}$, to state-dependent spinor energies $\varepsilon_p = \varepsilon_p(\nu)$. The intruder state avoidance approach[39] can also be implemented by changing the energy denominators to a form that always takes a nonzero value.

[1] H. J. Aa. Jensen, T. Saue, L. Visscher *et al.*, DIRAC 04, Release DIRAC04.0, a relativistic *ab initio* electronic structure program, 2004.
[2] L. Visscher, O. Visser, P. J. C. Aerts, H. Merenga, and W. C. Nieuwpoort, Comput. Phys. Commun. **81**, 120 (1994); L. Visscher, W. A. de Jong, O. Visser, P. J. C. Aerts, H. Merenga, and W. C. Nieuwpoort, in *Methods and Techniques for Computational Chemistry, METECC-5* edited by E. Clementi and G. Corongiu (STEF, Cagliari, 1995), pp. 169–218.
[3] H. Nakano, J. Chem. Phys. **99**, 7983 (1993).
[4] H. Nakano, Chem. Phys. Lett. **207**, 372 (1993).
[5] K. Hirao, Chem. Phys. Lett. **190**, 374 (1992).
[6] K. Hirao, Chem. Phys. Lett. **196**, 397 (1992).
[7] K. Hirao, Int. J. Quantum Chem. **S26**, 517 (1992).
[8] H. Nakano, R. Uchiyama, and K. Hirao, J. Comput. Chem. **23**, 1166 (2002).
[9] H. Nakano, J. Nakatani, and K. Hirao, J. Chem. Phys. **114**, 1133 (2001).
[10] M. J. Vilkas, K. Koc, and Y. Ishikawa, Chem. Phys. Lett. **296**, 68 (1998).
[11] R. K. Chaudhuri and K. F. Freed, J. Chem. Phys. **122**, 204111 (2005).
[12] K. Freed, *Lecture Notes in Chemistry* (Springer, Berlin, 1989), Vol. 52, p. 1, and references therein.
[13] M. J. Vilkas and Y. Ishikawa, Phys. Rev. A **69**, 062503 (2004).
[14] M. J. Vilkas and Y. Ishikawa, Phys. Rev. A **72**, 032512 (2005).
[15] I. Shavitt and L. R. Redmon, J. Chem. Phys. **73**, 5711 (1980), and references therein.
[16] T. Fleig, J. Olsen, and L. Visscher, J. Chem. Phys. **119**, 2963 (2003).
[17] I. Lindgren and J. Morrison, *Atomic Many-Body Theory* 2nd ed. (Springer, Berlin, 1985).
[18] S. Zarrabian, C. R. Sarma, and J. Paldus, Chem. Phys. Lett. **155**, 183 (1989).
[19] R. J. Harrison and S. Zarrabian, Chem. Phys. Lett. **158**, 393 (1989).
[20] M. Abe, H. Iikura, M. Kamiya, T. Nakajima, S. Yanagisawa, and T. Yanai, REL4D.
[21] T. Yanai, M. Kamiya, Y. Kawashima *et al.*, UTCHEM 2004.
[22] K. G. Dyall, Theor. Chem. Acc. **108**, 335 (2002).
[23] K. P. Huber and G. Herzberg, *Molecular Spectra and Molecular Structure IV: Constants of Diatomic Molecules* (Van Nostrand Reinhold, New York, 1979).
[24] L. Visscher, E. Eliav, and U. Kaldor, J. Chem. Phys. **115**, 9720 (2001).
[25] K. Balasubramanian and J. Li, J. Mol. Spectrosc. **135**, 169 (1989).
[26] J. M. L. Martin and A. Sundermann, J. Chem. Phys. **114**, 3408 (2001).
[27] A. Bergner, M. Dolg, W. Kuechle, H. Stoll, and H. Preuss, Mol. Phys. **80**, 1431 (1993).
[28] T. Koga, H. Tatewaki, and O. Matsuoka, J. Chem. Phys. **115**, 3561 (2001).
[29] T. H. Dunning, Jr., J. Chem. Phys. **90**, 1007 (1989).
[30] D. Ajitha, D. G. Fedorov, J. P. Finley, and K. Hirao, J. Chem. Phys. **117**, 7068 (2002).
[31] D. G. Fedorov and J. P. Finley, Phys. Rev. A **64**, 042502 (2001).
[32] A. Gedanken and M. D. Rowe, Chem. Phys. Lett. **34**, 39 (1975).
[33] R. A. Kendall, T. H. Dunning, Jr., and R. J. Harrison, J. Chem. Phys. **96**, 6796 (1992).
[34] D. E. Woon and T. H. Dunning, Jr., J. Chem. Phys. **98**, 1358 (1993).
[35] A. K. Wilson, D. E. Woon, K. A. Peterson, and T. H. Dunning, Jr., J. Chem. Phys. **110**, 7667 (1999).
[36] National Institute of Standards and Technology (NIST), Atomic Spectra Database, http://physics.nist.gov/PhysRefData/ASD/ and references therein.
[37] A. Zaitsevskii and J. P. Malrieu, Chem. Phys. Lett. **233**, 597 (1995).
[38] A. Zaitsevskii and J. P. Malrieu, Chem. Phys. Lett. **250**, 366 (1996).
[39] H. A. Witek, Y.-K. Choe, J. P. Finley, and K. Hirao, J. Comput. Chem. **23**, 957 (2002).